Chemistry as a function of the fine-structure constant and the electron-proton mass ratio

Rollin A. King

Department of Chemistry, Bethel University, St. Paul, Minnesota 55112, USA

Ali Siddiqi, Wesley D. Allen, and Henry F. Schaefer III

Department of Chemistry and Center for Computational Chemistry, University of Georgia, Athens, Georgia 30602, USA

In standard computations in theoretical quantum chemistry the accepted values of the fundamental physical constants are assumed. Alternatively, the tools of computational quantum chemistry can be used to investigate hypothetical chemistry that would result from different values of these constants, given the same physical laws. In this work, the dependence of a variety of basic chemical quantities on the values of the fine-structure constant and the electron-proton mass ratio is explored. In chemistry, the accepted values of both constants may be considered small, in the sense that their increase must be substantial to seriously impact bond energies. It is found that if the fine-structure constant were larger, covalent bonds between light atoms would be weaker, and the dipole moment and hydrogen-bonding ability of water would be reduced. Conversely, an increase in the value of the electron-proton mass ratio increases dissociation energies in molecules such as H_2, O_2, and CO_2. Specifically, a sevenfold increase in the fine-structure constant decreases the strength of the O–H bond in the water molecule by 7 kcal mol^{-1} while reducing its dipole moment by at least 10%, whereas a 100-fold increase in the electron-proton mass ratio increases the same bond energy by 11 kcal mol^{-1}.

PACS number(s): 31.15.A−, 31.15.B−, 31.15.X−, 31.30.J−

I. INTRODUCTION

In the 1950s Hoyle discovered that unless the reaction $3\,^4\text{He} \rightarrow {}^{12}\text{C} + 2\gamma$ is promoted by a precise positioning of nuclear energy levels, negligible carbon would be produced in stellar nucleosynthesis [1,2]. Without this "triple α resonance" process for creating ^{12}C nuclei in stars, no carbon-based life would be possible in the universe. In actuality, a spectacular chain of occurrences is responsible for carbon formation—the anomalously long lifetime of ^{8}Be compared to the ^{4}He + ^{4}He collision time, the presence of an excited nuclear state of ^{12}C within 60 keV of 7.644 MeV, and the downshift of a similar ^{16}O level (7.1187 MeV) to a point just below the total energy of ^{12}C + ^{4}He (7.1616 MeV) [3,4].

In the past half-century, such discoveries in physics and cosmology have established fine-tuning investigations regarding the physical laws of our universe as fertile domains of inquiry [5]. For example, Oberhummer *et al.* [6] used stellar model calculations to show that "outside a narrow window of 0.5 and 4% of the values of the strong and Coulomb forces, respectively, the stellar production of carbon or oxygen is reduced by factors of 30 to 1000." It is generally agreed upon that the existence of (at least) carbon-based life depends sensitively on the values of the fundamental physical constants [7]. It is unclear whether a "theory of everything" should predict the values of the constants or perhaps just a probability distribution for them, but Barrow [8] writes, "We need to know all those constants of Nature whose values provide necessary conditions for the existence of observers."

Does an equivalent of the "triple α resonance" exist in *chemistry*? This difficult question has not been seriously explored. However, the tools of computational molecular quantum mechanics may be used to mathematically determine alternative chemistries resulting from precise but varied physical laws. The simplest variation is the consideration of chemistry governed by the known physical laws with alternative values of the physical constants. Of particular significance, such investigations promise to reveal the realm of possibilities for the chemical fabric of biological complexity (i.e., whether life could exist if chemistry were appreciably different in various ways).

A. Nonrelativistic chemistry and the Schrödinger equation

The chemistry of [H, C, N, O], constituting the basis for biology, is governed to very high accuracy by the Schrödinger equation. For a general system of nuclei and electrons, the time-independent, nonrelativistic Schrödinger equation for a many-particle wave function Ψ and system energy E is

$$\left[-\frac{\hbar^2}{2} \sum_I \frac{1}{M_I} \nabla_I^2 - \frac{\hbar^2}{2m_e} \sum_i \nabla_i^2 + e^2 \sum_{I>J} \frac{Z_I Z_J}{r_{IJ}} \right.$$
$$\left. - e^2 \sum_{I,i} \frac{Z_I}{r_{Ii}} + e^2 \sum_{i>j} \frac{1}{r_{ij}} \right] \Psi = E\Psi, \tag{1}$$

where (I, J) and (i, j) are indices for nuclei and electrons, respectively, with attendant masses M_I and m_e, the Z_I are nuclear charges, and r_{IJ}, r_{Ii}, and r_{ij} denote nuclear-nuclear, nuclear-electron, and electron-electron distances, in order. Nonrelativistic, *ab initio* quantum chemistry mathematically determines the structures, properties, thermochemistry, and reactivities of molecules by directly converging on numerical solutions of Eq. (1) without empirical parametrization. The dramatic advances of recent decades in electronic structure methods, numerical algorithms, and raw computing power permit the determination of solutions very close to the *ab initio* limit for molecular systems of reasonable size.

In order to factor out the dependence of the Schrödinger equation on fundamental constants, a scaling of (distances, energies) in Eq. (1) to atomic units $[a_0 = \hbar^2(m_e e^2)^{-1}, E_h = m_e e^4 \hbar^{-2}]$ is ubiquitously employed, yielding

$$\left[-\frac{1}{2} \sum_I \frac{\beta}{\mu_I} \nabla_I^2 - \frac{1}{2} \sum_i \nabla_i^2 + \sum_{I>J} \frac{Z_I Z_J}{\rho_{IJ}} - \sum_{I,i} \frac{Z_I}{\rho_{Ii}} \right.$$
$$\left. + \sum_{i>j} \frac{1}{\rho_{ij}} \right] \Psi = \varepsilon \Psi, \qquad (2)$$

in which the energy (ε) and distance (ρ) variables are now unitless, μ_I is the ratio of nuclear mass I to the mass of the proton (m_p), and $\beta = m_e/m_p \approx 1/1836$. Because $\beta \ll 1$ (and $\mu_I \geqslant 1$), nuclear and electronic motions have disparate classical time scales, a wide separation in velocities that has profound consequences for chemistry. A vivid picture of this principle is that the fast electrons instantaneously adjust to the slow nuclear motions like "flies on an ox."

This time-scale separation is mathematically embodied in the highly accurate Born-Oppenheimer approximation, whereby the electronic part of the Schrödinger equation is first solved with clamped nuclei,

$$\hat{H}_0 \Psi_e \equiv \left[-\frac{1}{2} \sum_i \nabla_i^2 + \sum_{I>J} \frac{Z_I Z_J}{\rho_{IJ}} - \sum_{I,i} \frac{Z_I}{\rho_{Ii}} + \sum_{i>j} \frac{1}{\rho_{ij}} \right] \Psi_e$$
$$= \varepsilon_e(\boldsymbol{\rho}_{\text{nuc}}) \Psi_e, \qquad (3)$$

yielding a potential energy surface $\varepsilon_e(\boldsymbol{\rho}_{\text{nuc}})$ for motion of the nuclei as a function of the scaled positions $\boldsymbol{\rho}_{\text{nuc}}$. The resulting nuclear wave equation is then solved for the final rovibronic energy levels (ε):

$$\left[-\frac{1}{2} \sum_I \frac{\beta}{\mu_I} \nabla_I^2 + \varepsilon_e(\boldsymbol{\rho}_{\text{nuc}}) \right] \Psi_{\text{nuc}} = \varepsilon \Psi_{\text{nuc}}. \qquad (4)$$

The topography of the surface $\varepsilon_e(\boldsymbol{\rho}_{\text{nuc}})$ provides the basis for ascribing geometric structures to molecules. The local minima occurring on this multidimensional surface correspond to the pervasive three-dimensional molecular structures of chemistry, on which virtually all chemical intuition is built. The implicit assumption made in drawing static molecular frameworks is that the nuclei are localized in wells centered about such structures and execute only small-amplitude vibrations away from their equilibrium positions.

The solutions to the scaled electronic Schrödinger equation are pure numbers independent of the fundamental constants. The conversion factors between atomic and (macroscopic) SI units then relate these solutions to laboratory observations. Observational distinguishability from our known universe occurs only by changing dimensionless ratios of fundamental constants [9].

B. Influence of the fine-structure constant and the electron-proton mass ratio

The dimensionless ratios that have consequences for chemistry are the fine-structure constant $[\alpha = e^2/(\hbar c)]$ and the electron-proton mass ratio (β). In conventional, nonrelativistic quantum chemistry within the Born-Oppenheimer approximation, it is assumed that both ratios are negligibly small. The most important relativistic effects in chemistry can be investigated by means of the Cowan-Griffin Hamiltonian [10] in which $\hat{H}_0$ in Eq. (3) is augmented with one-electron mass-velocity and Darwin terms:

$$\hat{H}_1 = \alpha^2 \left[-\frac{1}{8} \sum_i \nabla_i^4 + \frac{\pi}{2} \sum_{I,i} \delta(\rho_{Ii}) \right], \qquad (5)$$

where α is the fine-structure constant, and $\delta(\rho_{Ii})$ is a Dirac delta function of the nuclear-electron distances. The incorporation of $\hat{H}_1$ by means of perturbation theory is often of sufficient accuracy as long as α is much less than 1. It may be expected that lighter elements (such as H, C, N, or O) will become more relativistic as α is increased.

The consequences of finite m_e/m_p ratios on chemical systems can be probed by means of the diagonal Born-Oppenheimer correction (DBOC) [11,12]

$$E_{\text{DBOC}} = -\frac{\beta}{2} \sum_I \frac{1}{\mu_I} \langle \Psi_e | \nabla_I^2 | \Psi_e \rangle. \qquad (6)$$

The E_{DBOC} term gives a first-order correction to the Born-Oppenheimer approximation while maintaining the concept of potential energy surfaces for nuclear motion and hence molecular geometric structures.

Barrow has roughly sketched out the cosmological habitable zone in the (α, β) plane for the existence of life-supporting complexity [13]. However, no previous work has applied rigorous computational methods to the *chemistry* of this problem. We investigate here the chemical effects induced by variation of α and β in Eqs. (5) and (6) by means of computations on numerous essential model systems, including diatomic molecules; the molecular structure, hydrogen-bonding ability, and dipole moment of water; hydrocarbons; and combustion reactions.

II. THEORETICAL METHODS

Molecular energies and structures were determined including the one-electron mass-velocity and Darwin (MVD) operators in Eq. (5) by using electron densities from spin-restricted Hartree-Fock and more robust coupled cluster singles and doubles (CCSD) wave functions [14]. Our principal approach followed that of established perturbative techniques [10,15,16], except with a critical new feature—allowance for variation of the fine-structure constant from the standard value $\alpha_\text{o} = 1/137.0359997$ [17].

Initial chemical results for increasing values of α showed that standard one-electron Gaussian basis sets commonly used in electronic structure theory are deficient in this new realm, and thus an extensive study of basis-set dependencies was executed. Consideration of basis-set economy, the quality of chemical results, and suitability for correlated electronic wave functions led us to adopt a C, N, O $(10s6p2d1f)$ and H $(3s2p)$ Gaussian atomic-orbital basis, derived from a TZ$(2d1f, 2p)$ polarized triple-ζ (TZ) set we have used in earlier work [18] by fully uncontracting (U) the basis functions on all atoms but hydrogen. We denote this basis set "U-TZ$(2d1f, 2p)$" and have used it for myriad computations

with counterfactual values of α. The RHF + MVD and CCSD + MVD computations were carried out using the PSI3 program package [19].

The validity of our cost-effective MVD approaches for wide-ranging surveys of counterfactual chemistry was established by performing several types of relativistic computations whose accuracy does not deteriorate for large values of α. Douglas-Kroll-Hess (DKH) results [20] were obtained with the NWCHEM package, by changing the assumed speed of light to effectively insert nonstandard values of α. Likewise, the DIRAC08 [21] program was used to obtain results with several other relativistic Hamiltonians in conjunction with CCSD(T) wave functions [22–24], including the two-component Hamiltonian obtained after the Barysz-Sadlej-Snijders (BSS) transformation of the Dirac Hamiltonian with scalar and spin-orbit effects up to infinite order [25], the four-component Dirac-Coulomb Hamiltonian (4C-DC), and the one-step exact (infinite order) two-component Hamiltonian (X2C) [26]. For these DIRAC08 computations all basis sets (including those on H atoms) were fully uncontracted, including fully uncontracted versions of the aug-cc-pVTZ, cc-pVQZ, and cc-pV5Z basis sets [27,28], denoted U-aug-cc-pVTZ, U-cc-pVQZ, and U-cc-pV5Z, respectively. As shown in the discussion to follow, for the structure of the water molecule, the U-TZ($2d1f, 2p$) RHF + MVD predicted shifts are quantitatively accurate up to $\alpha/\alpha_o \approx 8$ and qualitatively correct thereafter.

We also implemented a scheme for estimating the effects of quantum electrodynamics (QED) as the fine-structure constant is increased. With the natural value of α, QED has virtually no effect on chemistry, but this is not necessarily the case for counterfactual conditions. An approximation (E_{QED}) to the largest self-energy and vacuum-polarization contributions to the energy of an electron in a Coulomb field from quantum electrodynamics can be achieved by renormalizing the one-electron Darwin energy (E_{D1}) according to [29]

$$\frac{E_{QED}}{E_{D1}} = \frac{2\alpha}{\pi}\left[F(Z\alpha) - \frac{4}{15}\right]. \tag{7}$$

Values of the function $F(Z\alpha)$ have been tabulated for one-electron systems by Mohr and co-workers [30] and have a small dependence on the principal quantum number n. We have used the $n = 1$ and $l = 0$ values for each atom. The function $F(Z\alpha)$ continuously decreases from $F(\alpha_o) = 10.3168$ to $F(110\alpha_o) = 1.660$. For a few computations at still higher domain values, we have assumed the latter value of 1.660. In effect, the contribution of each nucleus to the Darwin term in Eq. (5) is scaled by the factor on the right side of Eq. (7) to obtain an additional QED correction to the total energy. Summing over all nuclei yields the scheme we denote as MVD + QED(1). The use of atomic contributions from Eq. (7) to estimate QED effects on molecular potential energy surfaces has been proposed earlier by Pyykkö and co-workers [29].

To explore counterfactual quantum chemistry for larger electron-proton mass ratios, the DBOC method of Eq. (6) for arbitrary values of β was implemented within the PSI3 package [19]. To make broad explorations of β effects feasible, E_{DBOC} was computed with Hartree-Fock electronic wave functions utilizing standard cc-pVTZ basis sets [27]. The use of Hartree-Fock DBOCs for high-accuracy thermochemical computations with the standard value $\beta_o = 1/1836.152672$ [17] is well established [31].

III. RESULTS

A. Structure of the water molecule

The equilibrium bond angle and bond length of the water molecule as a function of α are shown in Figs. 1 and 2, respectively. As expected, the structure of water in the natural
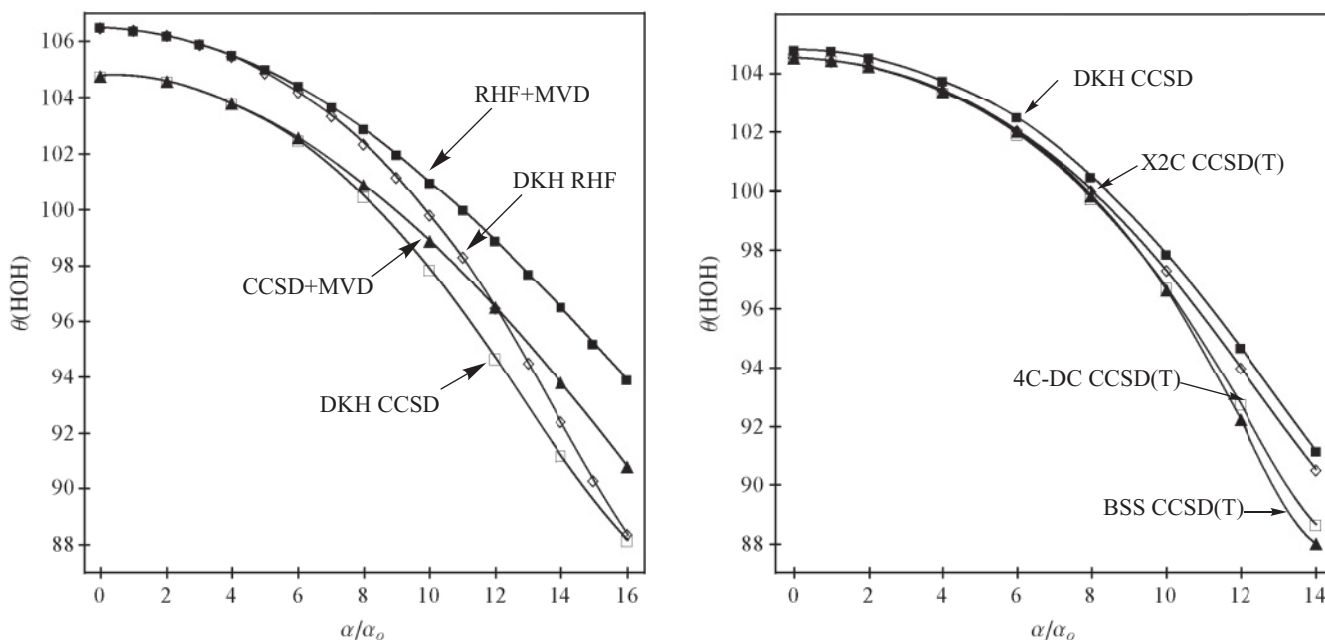

FIG. 1. Bond angle (degrees) of the water molecule as a function of the fine-structure constant, computed with the U-TZ($2d1f, 2p$) basis set.
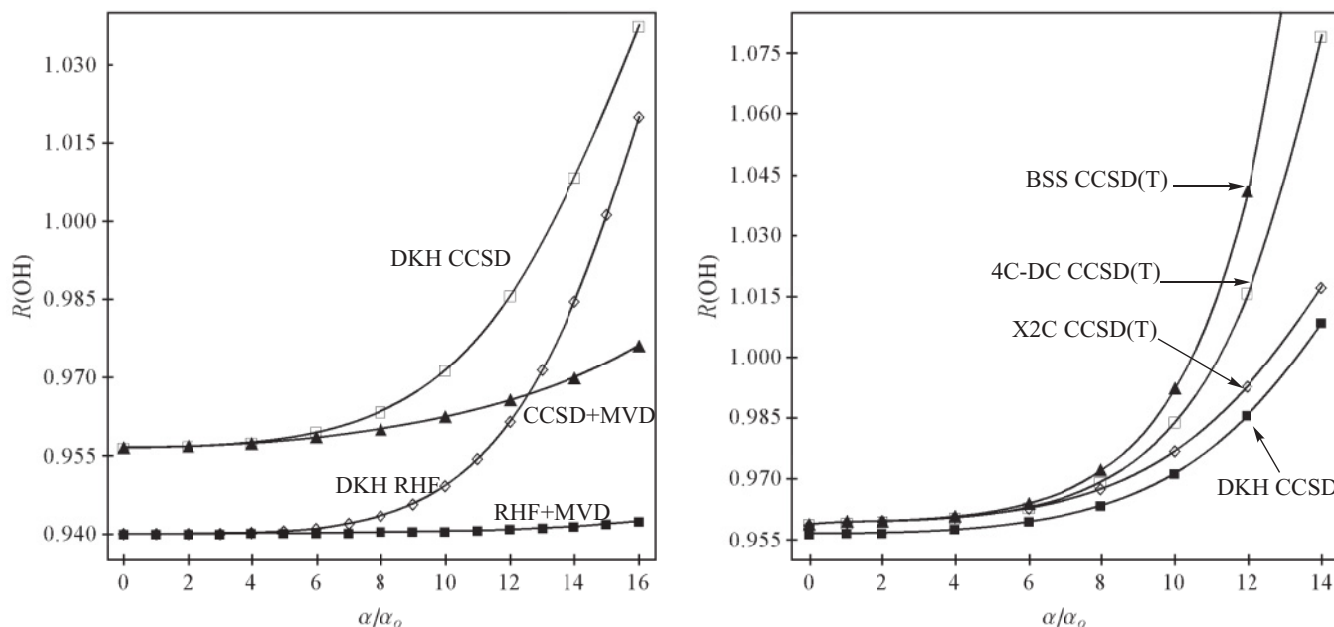
FIG. 2. Bond length (Å) of the water molecule as a function of the fine-structure constant, computed with the U-TZ($2d1f$, $2p$) basis set.

world ($\alpha/\alpha_o = 1$) is near the asymptotic limit for small α. All theoretical methods predict a substantial and continuous decrease in the bond angle with increasing α. Of the less computationally costly methods (shown in the left panel), the DKH CCSD method should provide the most accurate predictions. Beyond $\alpha/\alpha_o \approx 4$, the angle decreases rapidly, reaching 90° as $\alpha \rightarrow 15\alpha_o \approx 0.11$ in the DKH RHF and DKH CCSD curves. Note that the difference between the MVD and DKH bond-angle results is reduced by including CCSD electron correlation. For $\alpha/\alpha_o < 8$, there is no significant change in the O–H distance in water (Fig. 2); however, further increase in α causes a rapid elongation of the bond, particularly in the more rigorous DKH predictions.

The adequacy of using the DKH CCSD results as benchmarks was tested in several ways. The right panels of Figs. 1 and 2 present the structure of the water molecule computed with several relativistic Hamiltonians (and also including a perturbative correction for connected triple excitations in the treatment of electron correlation). The predicted trends with respect to α are similar, with the DKH CCSD results providing a lower bound to the impact of increasing the value of the fine-structure constant. The greatest sensitivity with respect to α is predicted by the BSS CCSD(T) method, so that method was chosen to test the adequacy of the one-electron basis set. Plots of the geometrical parameters for the water molecule as a function of basis set are provided as supplementary material (auxiliary figures), where increasing the basis-set size up to U-cc-pV5Z is seen to make essentially no difference to the predicted shifts [32].

These structural results show that substantially increasing α would have dramatic consequences on the physical characteristics of water. With the natural value of α, each molecule in liquid water ideally forms four hydrogen bonds that are roughly tetrahedrally arranged, such that local clustering expands the volume and decreases the density. As α increases and the water bond angle is reduced substantially below the

tetrahedral value, the hydrogen-bonded network is disrupted. Accordingly, the density of ice will no longer be less than that of liquid water, and one of the unique characteristics of H_2O could be lost. This change has profound consequences, as recognized in the early life-fitness inquiries of Henderson [33].

The total MVD relativistic energy correction arises from the negative MV term being larger in magnitude than the positive D contribution. For the natural value of $\alpha/\alpha_o = 1$, the QED correction adds only $\sim 2\%$ to the normal Darwin energy (E_{D1}) of the water molecule. However, E_{QED} increases as α^3 and will provide more cancellation of the MV energy for larger values of the fine-structure constant. Thus, it is expected that the additional QED term in Eq. (7) will somewhat diminish the effects of increasing α. For H_2O and $\alpha/\alpha_o = 10$, the QED correction rises to about 6% of E_{D1}. The consequences of QED on the bond angle of water are shown in Fig. 3, where the QED correction is seen to have a significant effect on the geometry of H_2O for α/α_o greater than ~ 10. The DKH and QED(1) improvements to the MVD curve are in opposite directions, and thus the unadorned MVD method seems to provide the best predictions owing to an advantageous cancellation of errors. The most important conclusion from Fig. 3 is that the large reduction of the bond angle with increasing α remains even when QED is considered.

The equilibrium structural parameters of water as a function of β at both the cc-pVTZ RHF and cc-pVTZ CCSD levels of theory are depicted in Figs. 4 and 5. In contrast to the analogous α results, the bond angle of water increases with increasing β. Nonetheless, the geometric changes are not substantial until β exceeds $100\beta_o \approx 0.054$, where a roughly 2° expansion of the bond angle is observed. The bond distance $R(OH)$ increases with β as in the α case, but the behavior is clearly linear rather than quadratic. At $100\beta_o$ the increase in $R(OH)$ is only 0.004 Å. Our data based on the DBOC approximation of Eq. (6) show no irregularities that would signal a catastrophic breakdown of this perturbation theory prior to $\beta = 400\beta_o \approx 0.2$. Thus,
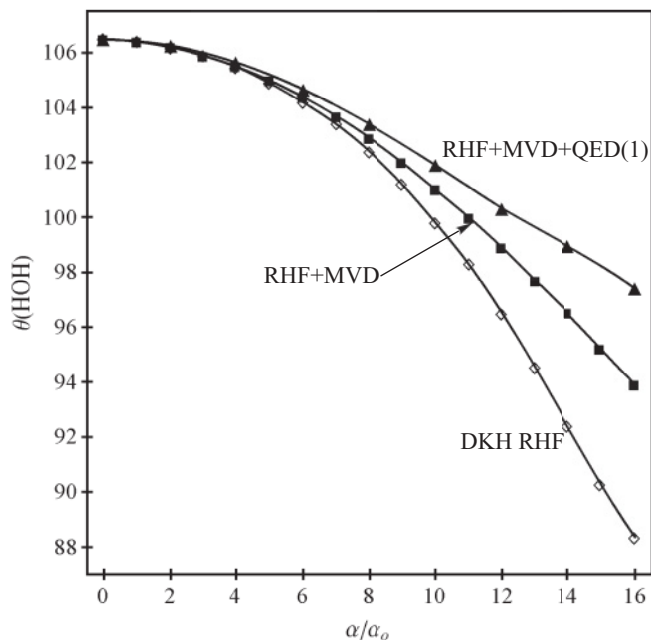
FIG. 3. QED and relativistic effects on the bond angle (degrees) of the water molecule as a function of the fine-structure constant, computed with the U-TZ($2d1f$, $2p$) basis set.

it appears that the important concept of molecular structure retains at least some validity even if the electron-proton mass ratio is increased a few hundred fold.

B. Thermochemistry of water and carbon π bonds

We have studied two reaction prototypes in detail in order to elucidate the consequences of the fine-structure constant on fundamental chemistry. The thermodynamic stability of the
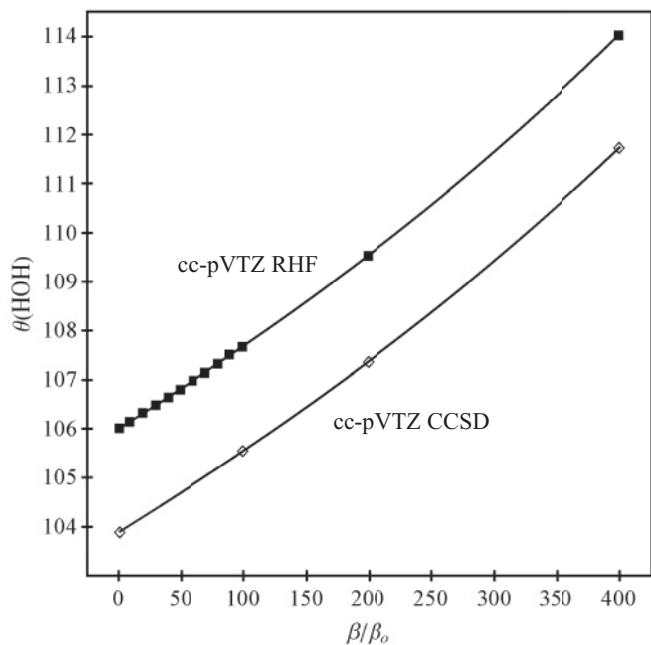
FIG. 4. Bond angle (degrees) of the water molecule as a function of the electron-proton mass ratio.
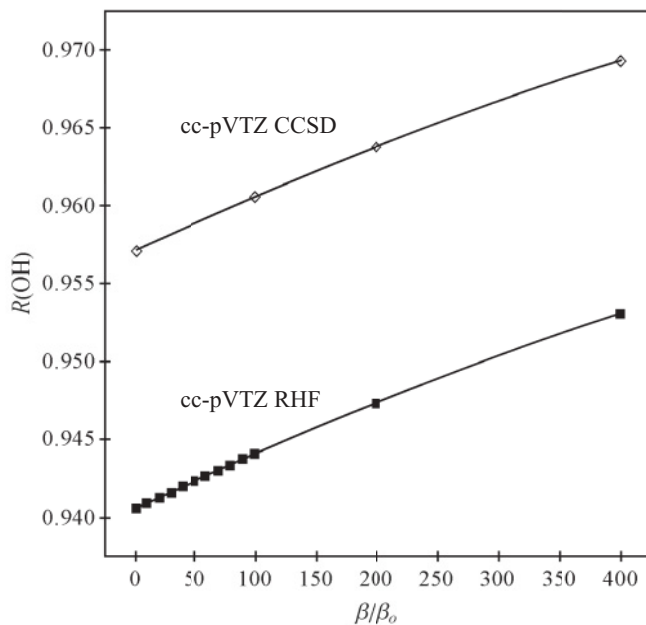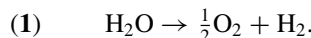

FIG. 5. Bond length (Å) of the water molecule as a function of the electron-proton mass ratio.

water molecule with respect to its elements is measured by the energy of the reaction

$$(1) \qquad H_2O \rightarrow \tfrac{1}{2}O_2 + H_2.$$

The relative strength of carbon-carbon π bonds, essential to the stabilization of DNA base pairs, *inter alia*, can be assessed from the energy of the acetylene/vinylidene isomerization
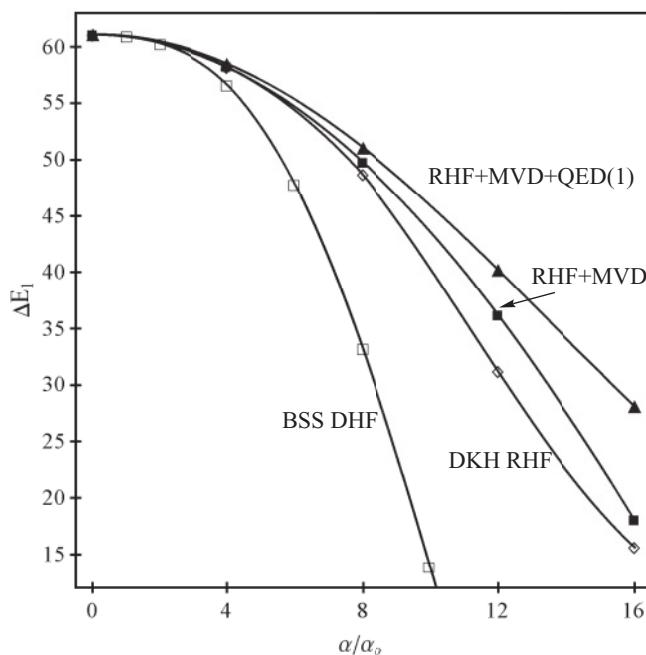
$$(2) \qquad HCCH \rightarrow H_2CC.$$

FIG. 6. Reaction energy (kcal mol^{-1}) for $H_2O \rightarrow \tfrac{1}{2} O_2 + H_2$ as a function of the fine-structure constant, computed with the U-TZ($2d1f$, $2p$) basis set.
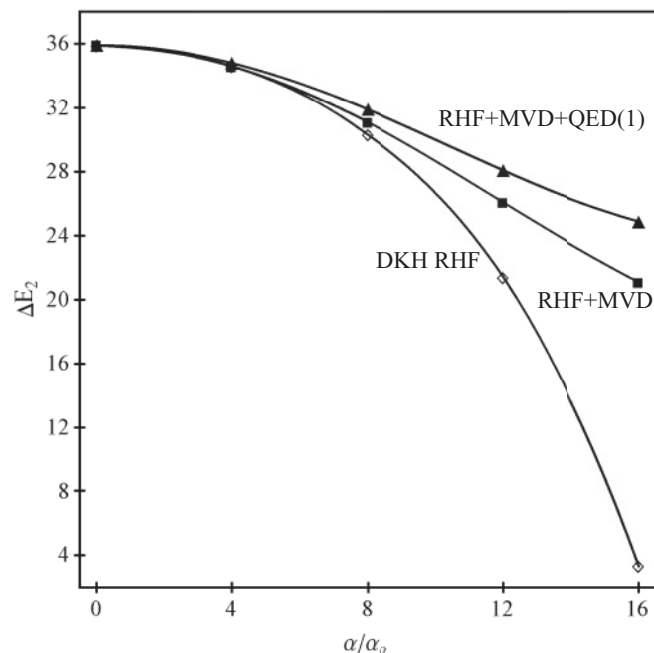
FIG. 7. Reaction energy (kcal mol^{-1}) for HCCH $\rightarrow$ H$_2$CC as a function of the fine-structure constant, computed with the U-TZ($2d1f$, $2p$) basis set.

FIG. 8. Reaction energy for H$_2$O $\rightarrow$ $\frac{1}{2}$O$_2$ + H$_2$ as a function of the electron-proton mass ratio.

The reaction energies for chemical transformations (**1**) and (**2**) have been determined by using both our MVD and DKH methods as a function of α. The data are shown in Figs. 6 and 7. For reaction (**1**) the nonrelativistic U-TZ($2d1f$, $2p$) CCSD(T) reaction energy is 60.2 kcal mol^{-1}, in comparison to the corresponding RHF value of 61.1 kcal mol^{-1}, showing that electron correlation does not substantially affect the thermochemistry in this case. Reaction energies computed with BSS DHF are also shown in Fig. 6, and these show a greater sensitivity to increasing α. The geometrical results for water would suggest that these values may serve as an upper bound to the magnitude of the true shifts with respect to increasing α.

The clear conclusion from Fig. 6 is that the thermodynamic stability of H$_2$O is reduced monotonically as relativity becomes more important. At $\alpha/\alpha_o = 4$, about 3 kcal mol^{-1} of the formation energy is lost. For $\alpha/\alpha_o = 8$, the loss in thermodynamic stability reaches at least 11 kcal mol^{-1}, a large fraction of the overall energy of reaction (**1**). The results in Fig. 7 suggest that π bonding in carbon compounds is less effective as α increases. For larger values of α, our preliminary conclusion is that divalent carbene species with lone electron pairs become increasingly more important in organic chemistry, even at low temperatures.

The β dependence of the thermodynamic stability of H$_2$O was also studied. The energy of reaction (**1**) at both the cc-pVTZ RHF and cc-pVTZ CCSD levels of theory is plotted versus β in Fig. 8. The consequences of increasing the electron-proton mass ratio are much greater for the reaction energy than for the geometric structure of H$_2$O. In particular, the thermodynamic stability of water increases significantly with increasing β, a phenomenon counter to the α effect. For $\beta/\beta_o = 100$ and 200, ΔE_1 increases by about 6 and 12 kcal
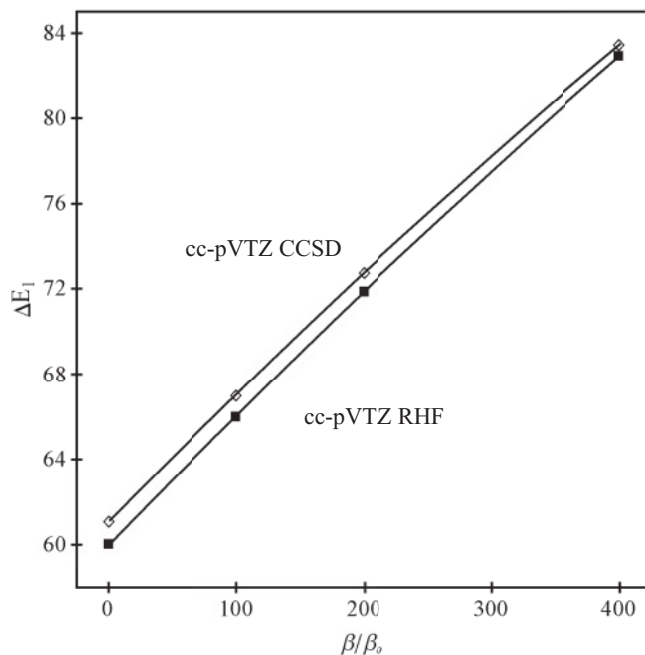
mol^{-1}, respectively, both amounts being sizable fractions of the total reaction energy.

C. The dipole moment and dimerization of the water molecule

The dipole moment of the water molecule as a function of the fine-structure constant was determined with the CCSD + MVD method by using finite differences of applied electric fields. The results are plotted in Fig. 9. The dipole moment of the optimized structure continuously decreases as α is increased, changing by more than 10% of its value by $\alpha/\alpha_o = 8$. The second panel of Fig. 9 shows that this reduction predicted by CCSD + MVD is probably a lower bound to the true difference (though, as shown earlier, the effects of QED may negate some of the increased sensitivity predicted by the more rigorous relativistic treatments).

Known structures of ice have fourfold- or tetra-coordinated oxygen atoms. Therefore, we also plot in the left panel of Fig. 9 dipole moments of H$_2$O obtained with a fixed tetrahedral bond angle of 109.47°. The two curves in the figure are very similar, indicating that the dipole moment reduction does *not* arise primarily from the geometric bond-angle contraction observed in Fig. 1, but from a fundamental reorganization of the electronic structure itself. The key conclusion from our dipole moment computations is that water becomes successively less polar as relativistic contributions are enhanced. Clearly,

TABLE I. Variation of the dimerization energy (kcal mol^{-1}) of H$_2$O with the fine-structure constant.

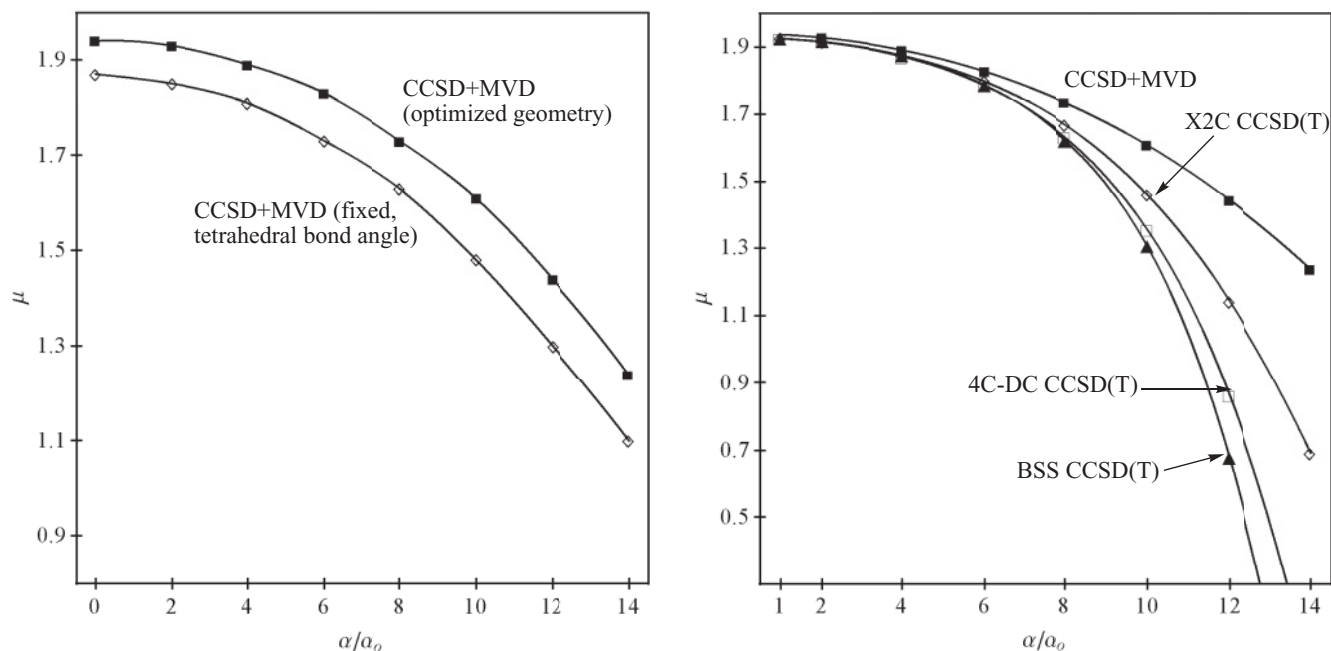| α/α_o	0	2	4	6	8	14
D_e	4.85	4.79	4.62	4.33	3.94	2.16

FIG. 9. Dipole moment (in Debyes) of the water molecule as a function of the fine-structure constant, computed using the U-TZ($2d1f, 2p$) basis set augmented with diffuse functions.

any significant decrease in the polarity of water would have far-reaching consequences on cell biology.

The variation of the dipole moment of H_2O with α suggests that the strength of hydrogen bonding in water is also likely to decrease as relativistic effects grow. We confirmed this expectation by explicit CCSD + MVD optimizations on the water dimer. For this purpose our standard U-TZ($2d1f, 2p$) basis was augmented with diffuse $O(sp)$ and $H(s)$ functions. As shown in Table I, increasing α to $6\alpha_o \approx 0.044$ decreases the dimerization energy of water by more than 10%. With $\alpha/\alpha_o = 14$, this hydrogen-bonding energy is less than half its natural value. While the precise relationship among the properties of the water molecule, the water dimer, and the macroscopic properties of water is the subject of ongoing research, it is clear that drastic changes to the macroscopic properties of water (its melting point, temperature of maximum density, solvating qualities, viscosity, etc.) would occur long before this point. The essential strength of the hydrogen bond in water puts bounds on the value of the magnitude of the fine-structure constant allowable for complex life, at least in forms that we can currently conceive.

D. Survey of thermochemical prototypes

Table II lists reaction energies for 30 thermochemical prototypes as a function of the fine-structure constant. These computations were executed at the CCSD + MVD level with our U-TZ($2d1f, 2p$) basis set at RHF + MVD optimized geometries. Some of the most noteworthy trends as α increases above its natural value are as follows: (1) Chemical bonds are generally weaker, and molecules are less stable to fragmentation; (2) the total combustion of hydrocarbons to $CO_2 + H_2O$ is much less exothermic; and (3) relativistic effects are substantial at $\alpha = 7\alpha_o \approx 0.051$ and often extreme at $\alpha = 14\alpha_o$

TABLE II. Variation of reaction energies (kcal mol^{-1}) with the fine-structure constant.

α/α_o	0	7	14
$F^- \rightarrow F + e^-$	60.4	48.5	12.9
$H_2 \rightarrow 2H$	106.2	107.3	107.0
$O_2 \rightarrow 2O$	102.5	92.3	62.6
$F_2 \rightarrow 2F$	24.6	22.6	17.7
$CH_4 \rightarrow CH_3 + H$	109.7	108.6	105.4
$C_3H_8 \rightarrow CH_3CH_2CH_2 + H$	107.1	106.0	102.8
$H_2O \rightarrow H + OH$	120.0	112.8	92.6
$CH_3OH \rightarrow CH_3O + H$	108.2	101.2	81.7
$CH_3F \rightarrow CH_3 + F$	107.7	97.1	65.2
$HOOH \rightarrow 2OH$	44.8	38.0	22.8
$H_2O \rightarrow H_2 + \frac{1}{2}O_2$	63.5	53.9	29.7
$CO_2 \rightarrow CO + O$	119.0	102.4	51.7
$CO_2 \rightarrow CO + \frac{1}{2}O_2$	67.8	56.3	20.4
$H_2CO \rightarrow CO + H_2$	5.0	−5.0	−32.5
$HCCH \rightarrow H_2CC$	43.5	39.8	31.0
$CH_3NH_2 \rightarrow CH_3 + NH_2$	86.8	80.1	61.9
$C_2H_6 \rightarrow CH_3 + CH_3$	93.4	91.0	84.1
$C_3H_8 \rightarrow CH_3CH_2 + CH_3$	92.2	90.2	84.3
$C_3H_8 \rightarrow C_2H_4 + CH_4$	23.5	20.5	10.9
$C_2H_4 \rightarrow HCCH + H_2$	50.4	46.6	37.1
$C_2H_6 \rightarrow C_2H_4 + H_2$	41.3	37.2	27.5
$CH_3CH_2OH \rightarrow C_2H_4 + H_2O$	14.9	12.2	3.5
$CH_3COOH \rightarrow CH_3OH + CO$	28.1	19.5	−7.4
$CH_4 + 2O_2 \rightarrow CO_2 + 2H_2O$	−192.1	−169.8	−104.6
$C_2H_6 + \frac{7}{2}O_2 \rightarrow 2CO_2 + 3H_2O$	−340.4	−304.5	−199.3
$C_3H_8 + 5O_2 \rightarrow 3CO_2 + 4H_2O$	−486.8	−437.1	−290.9
$C_2H_6 + \frac{1}{2}O_2 \rightarrow C_2H_5OH$	−37.1	−28.9	−5.7
iso-$C_4H_{10} \rightarrow$ n-C_4H_{10}	1.3	1.6	2.3
propene $\rightarrow$ cyclopropane	7.4	10.4	20.7
2-butene $\rightarrow$ cyclobutane	7.4	9.7	17.9

TABLE III. Variation of reaction energies (kcal mol^{-1}) with the electron-proton mass ratio.

β/β_o	1	100	200	400
$H_2O \rightarrow H_2 + \frac{1}{2}O_2$	62.9	68.9	74.7	85.4
$H_2O \rightarrow H + OH$	122.2	133.0	143.8	165.2
$O_2 \rightarrow 2O$	105.1	106.2	107.4	109.8
$CO_2 \rightarrow CO + O$	121.5	121.8	122.1	122.6
$CO_2 \rightarrow CO + \frac{1}{2}O_2$	69.0	68.7	68.4	67.7
$H_2 \rightarrow 2H$	108.4	113.9	119.7	132.7

≈ 0.102. In addition, a few of the specific cases are particularly instructive. While it is not surprising that the bond energy in H_2 is insensitive to α, the reduction in the F_2 dissociation energy is surprisingly modest. In the $CH_4 \rightarrow CH_3 + H$ reaction, increasing α by a factor of 14 reduces the C–H dissociation energy by only 4%. However, the strength of the O–H bond as measured by the reaction $CH_3OH \rightarrow CH_3O + H$ decreases by 24% (similar to the decrease for water). Increasing the fine-structure constant to $\alpha/\alpha_\mathrm{o} = 7$ increases the strength of the C–H bond by 6 kcal mol^{-1} relative to the strength of the O–H bond, with profound implications for chemical reactions in which there is competition between these bond types.

For the $C_2H_6 \rightarrow CH_3 + CH_3$ fragmentation, 97.4% and 90.0% of the C–C bond energy is retained at $\alpha/\alpha_\mathrm{o} = 7$ and 14, respectively. Therefore, the ability of carbon to concatenate is not destroyed for large increases in α, even while C–O and O–O bonds are greatly weakened. It was also found that the energy of the reaction $C_6H_6 + 6CH_4 \rightarrow 3CH_3CH_3 + 3CH_2CH_2$ commonly used to measure the delocalization energy in benzene is remarkably insensitive to changes in α, with values (obtained from CCSD + MVD optimized geometries) increasing from 57.6 kcal mol^{-1} in the nonrelativistic limit ($\alpha = 0$) to only 59.9 kcal mol^{-1} when $\alpha/\alpha_\mathrm{o} = 14$. In summary, the survey in Table II reveals rich and sometimes unexpected variations of chemistry with α, suggesting that many interesting phenomena are yet to be discovered.

Finally, Table III collects reaction energies for several of our thermochemical prototypes as a function of the electron-proton mass ratio. These computations employed all-electron cc-pVTZ CCSD electron-correlated Born-Oppenheimer energies conjoined with β-dependent DBOC energies obtained at the cc-pVTZ RHF level. The necessary geometric structures for this dataset were optimized with the same method. Not surprisingly, reactions in which bonds are broken and formed among heavy atoms exhibit only weak dependence on β. In contrast, bonds involving a hydrogen atom are substantially strengthened as β increases. The strongest example of this phenomenon in Table III is $H_2O \rightarrow H + OH$, for which the dissociation energy increases by 11 and 22 kcal mol^{-1} for $\beta/\beta_\mathrm{o} = 100$ and 200, respectively.

IV. CONCLUSIONS

Two dimensionless ratios involving fundamental physical constants have direct consequences for chemistry: the fine-structure constant [$\alpha = e^2/(\hbar c)$] and the electron-proton mass ratio ($\beta = m_e/m_p$). The quantum chemistry of [H, C, N, O], forming the foundation of biochemistry, corresponds closely to the limit in which both α and β are negligibly small. By exploring the counterfactual chemistry created by alternative values of α and β, *ab initio* quantum chemical methods can probe the cosmological habitable zone for the existence of life-supporting complexity. Our theoretical research extends the previous substantial research on the fine-tuning of physical constants necessary for our current existence into the realm of chemistry.

Numerous model systems were investigated by our computational methods to elucidate the influence of α and β on chemistry. The findings for the water molecule exemplify some of the important (α, β) effects. The equilibrium bond angle in H_2O monotonically decreases as α increases, ultimately destroying the unique tetrahedral hydrogen-bonding capabilities that lead to the expansion of liquid water upon freezing. Increasing α also makes water significantly less polar and reduces its hydrogen-bond strength. The effect of increasing β is not so much in the geometric structure of H_2O but in the enhancement of the thermodynamic stability of water. This study indicates that large changes to chemical properties and reactivity, and consequently to biology, would result from significantly different values of the fine-structure constant and the electron-proton mass ratio. Nonetheless, the broad (α, β) sensitivity determined here for the chemistry of life-supporting molecules is not as spectacular as the narrow constraints on these fundamental constants established previously in physics and cosmology.

[1] F. Hoyle, D. N. F. Dunbar, W. A. Wenzel, and W. Whaling, Phys. Rev. **92**, 1095 (1953).

[2] F. Hoyle, Astrophys. J. Suppl. **1**, 121 (1954).

[3] J. D. Barrow and F. J. Tipler, *The Anthropic Cosmological Principle* (Oxford University Press, Oxford, 1986).

[4] M. Livio, D. Hollowell, A. Weiss, and J. W. Truran, Nature (London) **340**, 281 (1989).

[5] R. H. Dicke, Nature (London) **192**, 440 (1961).

[6] H. Oberhummer, A. Csótó, and H. Schlattl, Science **289**, 88 (2000).

[7] B. J. Carr and M. J. Rees, Nature (London) **278**, 605 (1979).

[8] J. D. Barrow, *New Theories of Everything* (Oxford University Press, Oxford, 2007), p. 135.

[9] J. D. Barrow, in *The Constants of Nature. From Alpha to Omega—the Numbers That Encode the Deepest Secrets of the Universe* (Pantheon Books, New York, 2002), p. 49.

[10] K. Balasubramanian, *Relativistic Effects in Chemistry: Part A, Theory and Techniques* (Wiley, New York, 1997).

[11] N. C. Handy, Y. Yamaguchi, and H. F. Schaefer, J. Chem. Phys. **84**, 4481 (1986).

[12] E. F. Valeev and C. D. Sherrill, J. Chem. Phys. **118**, 3921 (2003).

[13] J. D. Barrow, in *The Constants of Nature. From Alpha to Omega—the Numbers That Encode the Deepest Secrets of the Universe* (Pantheon Books, New York, 2002), p. 167.

[14] R. J. Bartlett and J. F. Stanton, Rev. Comput. Chem. **5**, 65 (1995); T. D. Crawford and H. F. Schaefer, *ibid.* **14**, 33 (2000).

[15] K. Balasubramanian, *Relativistic Effects in Chemistry: Part B, Applications* (Wiley, New York, 1997).

[16] S. A. Perera and R. J. Bartlett, Chem. Phys. Lett. **216**, 606 (1993).

[17] P. J. Mohr, B. N. Taylor, and D. B. Newell, J. Phys. Chem. Ref. Data **37**, 1187 (2008).

[18] R. A. King, W. D. Allen, B. Ma, and H. F. Schaefer III, Faraday Discuss. Chem. Soc. **110**, 23 (1998).

[19] T. D. Crawford, C. D. Sherrill, E. F. Valeev, J. T. Fermann, R. A. King, M. L. Leininger, S. T. Brown, C. L. Janssen, E. T. Seidl, J. P. Kenny, and W. D. Allen, J. Comput. Chem. **28**, 1610 (2007).

[20] M. Reiher and A. Wolf, J. Chem. Phys. **121**, 2037 (2004); **121**, 10945 (2004); R. Samzow, B. A. Hess, and G. Jansen, *ibid.* **96**, 1227 (1992); B. A. Hess, Phys. Rev. A **32**, 756 (1985); A. Wolf, M. Reiher, and B. A. Hess, in *Relativistic Electronic Structure Theory. Part 1. Fundamentals*, edited by P. Schwerdtfeger (Elsevier, Amsterdam, 2002), pp. 622–663; G. Jansen and B. A. Hess, Phys. Rev. A **39**, 6016 (1989).

[21] DIRAC, a relativistic *ab initio* electronic structure program, Release DIRAC08 (2008), written by L. Visscher, H. J. Aa. Jensen, and T. Saue, with new contributions from R. Bast, S. Dubillard, K. G. Dyall, U. Ekström, E. Eliav, T. Fleig,

A. S. P. Gomes, T. U. Helgaker, J. Henriksson, M. Iliaš, Ch. R. Jacob, S. Knecht, P. Norman, J. Olsen, M. Pernpointner, K. Ruud, P. Sałek, and J. Sikkema (see http://dirac.chem.sdu.dk).

[22] K. Raghavachari, G. W. Trucks, J. A. Pople, and M. Head-Gordon, Chem. Phys. Lett. **157**, 479 (1989).

[23] L. Visscher, T. J. Lee, and K. G. Dyall, J. Chem. Phys. **105**, 8769 (1996).

[24] M. Pernpointner and L. Visscher, J. Comput. Chem. **24**, 754 (2003).

[25] M. Iliaš, H. J. Aa. Jensen, V. Kello, B. O. Roos, and M. Urban, Chem. Phys. Lett. **408**, 210 (2005).

[26] M. Iliaš and T. Saue, J. Chem. Phys. **126**, 064102 (2007).

[27] T. H. Dunning Jr., J. Chem. Phys. **90**, 1007 (1989).

[28] R. A. Kendall, T. H. Dunning Jr., and R. J. Harrison, J. Chem. Phys. **96**, 6796 (1992).

[29] P. Pyykkö, K. G. Dyall, A. G. Császár, G. Tarczay, O. L. Polyansky, and J. Tennyson, Phys. Rev. A **63**, 024502 (2001).

[30] P. J. Mohr and Y.-K. Kim, Phys. Rev. A **45**, 2727 (1992); P. J. Mohr, *ibid.* **46**, 4421 (1992); P. Indelicato and P. J. Mohr, *ibid.* **58**, 165 (1998); U. D. Jentschura, P. J. Mohr, and G. Soff, Phys. Rev. Lett. **82**, 53 (1999); T. Beier, P. J. Mohr, H. Persson, and G. Soff, Phys. Rev. A **58**, 954 (1998).

[31] A. Tajti, P. G. Szalay, A. G. Császár, M. Kállay, J. Gauss, E. F. Valeev, B. A. Flowers, J. Vázquez, and J. F. Stanton, J. Chem. Phys. **121**, 11599 (2004).

[32] See supplementary material at http://link.aps.org/supplemental/10.1103/PhysRevA.81.042523 for geometrical parameters for various larger basis sets.

[33] L. J. Henderson, *The Fitness of the Environment* (reprinted by Harvard University Press, Cambridge, Massachusetts, 1970); L. J. Henderson, *The Order of Nature* (Harvard University Press, Cambridge, Massachusetts, 1917).